Quantifying the Importance of Soil Forming Factors Using Multivariate Soil Data at Landscape Scale

A. Eger[1], N. Koele[2], T. Caspari[1], M. Poggio[3†], K. Kumar[3], and O. R. Burge[4]

[1]Manaaki Whenua – Landcare Research, Soils & Landscapes, Lincoln 7608, New Zealand

[2]Manaaki Whenua – Landcare Research, Land Use & Ecosystems, Lincoln 7608, New Zealand

[3]Manaaki Whenua – Landcare Research, Land Use & Ecosystems, Palmerston North 4474, New Zealand

[4]Manaaki Whenua – Landcare Research, Ecosystems & Conservation, Lincoln 7608, New Zealand

Corresponding author: A. Eger (egera@landcareresearch.co.nz)

†current address: Helmholtz-Zentrum für Umweltforschung, Department of Soil System Science, 06120 Halle, Germany

Key Points:

- Quantifying the importance of different soil forming factors that change concomitantly at landscape scale (climate, parent material)
- Utilizing soils of an altitude gradient combined with proximal soil sensing data, multivariate statistics and Bayesian mixing modelling
- Parent material explains three times more soil data variation than climate despite being frequently omitted in modern digital soil mapping
-

Abstract

The role of soil forming factors (time, parent material, climate, biota, topography) on soil processes has commonly been studied using soil sequences where only one factor varies between sites. However, when multiple factors change, it becomes difficult to partition the importance of different soil forming factors for soil formation. We show for an altitudinal gradient how proximal sensing (portable XRF, Fourier-Transform Infrared [FTIR]), multivariate statistics and Bayesian mixing modelling can help to quantify the importance of two soil forming factors. First, we confirmed the existing qualitative soil-landscape model of concomitant shifts in parent material (greywacke loess to mafic volcanics) and climate (higher precipitation) with altitude, leading to increases in pedogenic oxides, soil carbon, and soil Fe, while Si concentrations and pH declined. Second, we applied a mixing model using immobile elements as parent material tracers to quantify the parent material contribution in soils across our gradient. Third, we conducted a variation analysis to determine how much variation in the soil FTIR spectra could be explained by parent material and climate. Parent material alone explained 31% of the variation, climate alone only 9%. However, if we had only considered climate as explanatory variable, it would have accounted for almost half of the total variation (41%) because of the strong interaction between climate and parent material, and therefore concealing the leading role of parent material. Given that parent material is often omitted in modern digital soil mapping, our results emphasize the importance of parent material as a predictor of spatial soil distribution.

1 Introduction

A soil at a given location is the result of the integrated effects of multiple soil-forming processes. This is generally represented by the soil forming factor approach, where these processes are represented by their controlling environmental factors: climate, parent material/lithology, biota, and topography acting collectively over time to define the characteristics of a soil (Jenny, 1941). More recently, this long-standing concept has been put into a spatial context as SCORPAN (soil, climate, organisms, relief/topography, parent material, age, space: relative spatial position), a framework that is widely used for modelling the spatial distribution of soils in modern digital soil mapping (McBratney et al., 2003): quantitative or qualitative spatial information representing the SCORPAN factors are used as covariates to predict the spatial distribution of soil properties or classes using statistical and other modelling methods (e.g., Heung et al., 2016; Ma et al., 2017; McBratney et al., 2003; Odgers et al., 2011; Zhang et al., 2020).

To understand the individual roles of soil forming factors to drive soil developmental trajectories and closely inter-related ecological processes, scientific focus has been on experimental settings where all but one of the soil-forming factors can be kept near-constant by substitution for location. Most common examples of such well-constrained systems are chronosequences (only time/age varies between sites) (e.g., Crews et al., 1995; Dorji et al., 2009; Eger et al., 2011; Maher et al., 2009; S.J. Richardson et al., 2004; Tonkin & Basher, 2001; S. Turner et al., 2017; Wardle et al., 2004), climosequences (only climate varies) (e.g., O. A. Chadwick et al., 2003; Dere et al., 2013; Dixon et al., 2016; Helfenstein et al., 2018; Riebe et al., 2004; B. L. Turner et al., 2018; Webb et al., 1986), toposequences (only topography varies) (e.g., Agbenin & Tiessen, 1994; Araújo et al., 2004; K. D. Chadwick & Asner, 2020; Porder et al., 2005; S.J. Richardson et al., 2008; Vitousek et al., 2003) or parent material sequences/paired

sites (e.g., Bazilevskaya et al., 2013; Hahm et al., 2014; Mage & Porder, 2013; Vitousek et al., 2016). These sequences have been a very powerful tool to understand fundamental processes of soil formation, biogeochemical cycling, and above and below-ground ecological change (e.g., rock/mineral weathering, soil nutrient cycles, plant succession/retrogression, soil microbiology). While scientifically important, such model systems are naturally rare. Instead, most terrestrial landscapes are much less constrained, such that multiple soil forming factors concomitantly change with location. Understanding the drivers of soil formation in such 'messy' spatial contexts and the formulation of empirically supported soil-landscape models is however vital for modern soil mapping approaches, since they rely on covariates that are structurally meaningful to predict soil characteristics at a given locale (Behrens & Viscarra Rossel, 2020; Meyer et al., 2019).

In our study we present a methodological approach to quantitatively disentangle the effect of two soil forming factors on a given soil pattern. Our approach takes advantage of the recent progress in soil proximal sensing methods (Fourier-Transform Infrared spectroscopy [FTIR], portable X-ray fluorescence [pXRF]) and their increasing applicability and accessibility in soil science with respect to faster sample turnaround, and lower analytical costs compared to conventional laboratory methods (Viscarra Rossel et al., 2011; Viscarra Rossel et al., 2010). Our case study uses soils along an altitudinal gradient, which represents both a change in parent material (from wind-blown sediment [loess from greywacke] to volcanic extrusive rocks), and in climate (from soils with an annual water deficit to soils that receive precipitation in excess of the potential evapotranspiration). Our study is opens new opportunities for improving our understanding of mechanistic drivers of soil variability at landscape-scale, and highlights the relevance of parent material specifically, a factor that is often neglected in modern soil mapping approaches.

2 Materials and Methods

Firstly, we use soil chemical and proximal sensing data (FTIR, pXRF) to confirm the qualitative description of the dual climate and parent material gradients at the site. Secondly, we perform a parent material mixing model and examine its consistency with the soil chemical properties. Thirdly, we assess the relative contributions of climate and parent material using variance partitioning, with the FTIR data to identify which of the two soil forming factors is more important for soil formation across our altitudinal gradient. All data used in the analysis and discussion can be found in the Supplementary material.

2.1 Study area

The study sites are located at the northern flanks of Banks Peninsula, South Island, New Zealand (Figure 1). The peninsula was constructed by a series of volcanic eruptions between 11 to 5.8 My ago and reaches a maximum altitude of 919 m asl. The volcanic lithology relevant for our study is dominated by alkaline volcanic rocks (hawaiite, basalt, tuff, conglomerates). Overall, the mineralogy is dominated by plagioclase (andesine, labradorite), sometimes co-dominant with clinopyroxene, and subdominant olivine and Fe-oxides, including Fe-Ti magnetite (Sewell, 1988a, 1988b; Sewell et al., 1993). Partially superimposed over the volcanic rocks is Late Quaternary wind-blown sediment (loess) that can reach up to 15 m depth at lower elevations (Sewell et al., 1993). The source lithology of the local loess is quartzofeldspathic

Triassic greywacke sandstone that dominates the bedrock geology of the eastern side of the Southern Alps. Erosion of these ranges in the Quaternary formed an extensive alluvial fan (Canterbury Plains), now partially submerged, in association with braided-river systems, acting as the loess source. The loess parent material is dominated by quartz, ~30% feldspars (albite, K-feldspar), and <10% of each muscovite and chlorite (Trangmar & Whitton, pers. communication; Jowett, 1995; Raeside, 1964). The loess cover in Banks Peninsula thins with altitude and increasing slope gradient, and is virtually absent above elevations of 500-600 m in our study area. Concomitantly with altitude, annual averages of precipitation (MAP), temperature (MAT) and Penman evapotranspiration (PET) change from ~600 mm/12.4°C/820 mm at sea-level to ~1300 mm/9.3°C/650 mm at 900 m asl (Andrew Tait, National Institute of Water and Atmospheric Research [NIWA], pers. communication, 2015). This climatic regime imposes an annual water deficit of over 200 mm per year at sea level (Leathwick et al., 2002; Ministry for the Environment, 2002).

Figure 1: The study sites are located in the South Island of New Zealand, in the northern part of Banks Peninsula. Aerial imagery and digital elevation model supplied by Land Information New Zealand under CC BY 4.0 (https://data.linz.govt.nz/layer/105027-canterbury-banks-peninsula-lidar-1m-dem-2018-2019/; https://data.linz.govt.nz/layer/53519-canterbury-03m-rural-aerial-photos-2015-2016/).

The changes of parent material and climate are reflected in the soil pattern as observed in the field (Griffiths, 1973; Manaaki Whenua - Landcare Research, 2020; Trangmar, 1986): Fine-grained soils (<2 mm particle size, mainly silt) from loess, often with fragipans and redox mottling, dominate at low elevations (typical soils: Immature/Argilic/Fragic Pallic Soil; New Zealand Soil Classification – Hapludalfs, Haplustalfs, Haplustepts, Fragiudepts; Soil Taxonomy) (Hewitt, 1993; Soil Survey Staff, 1999). As altitude and slope gradient increase, soils are formed in mixed loess-volcanic rock colluvia that normally comprise at least 5% volcanic rock fragments (typical soils: Melanic Brown Soil – mainly Dystrudepts, subdominant: Rocky Recent Soil – Lithic Udorthents). With further altitude increase, soils derived from volcanic rocks become dominant, containing variable proportions of rock fragments, clay and sand (typical: Mafic Melanic Soil – mainly Lithic/Typic Hapludoll, co-dominant: Rocky Recent Soil – Lithic Udorthents), depending on the nature of the soil-forming substrate (e.g., mobile slope deposits,

saprolite). A similar soil pattern has also been recognised for Otago Peninsula 300 km south (Leslie, 1973a, 1973b). Vegetation cover today is mainly pasture for low intensity sheep and cattle farming. Prior to anthropogenic landcover change podocarp-hardwood forests dominated the peninsula.

2.2 Data collection and soil analysis to confirm the altitudinal gradient

Soil data were collected from 11 soil sites across three transects (Figure 1). The transects were selected on the basis of reflecting the variability of the volcanic lithology, representing a larger spatial extent beyond a single catchment, and having landowner approval. The soils were described in the field and classified according to the New Zealand Soil Classification (Table 1). Climate data were based on the period 1981-2010; they were produced by first calculating the 30-year statistics at climate station locations with available data, followed by interpolation of these statistics onto a 500 m spatial resolution grid (Andrew Tait, NIWA, pers. communication, 2015). Topographic site data was derived from a 1 m resolution digital elevation model (https://data.linz.govt.nz/layer/105027-canterbury-banks-peninsula-lidar-1m-dem-2018-2019/). We targeted Pallic (loess parent material), Brown (mixed loess-volcanic parent material) and Melanic soils (volcanic parent material) as typical pedons for the elevation gradient. We choose soils that we could core to 1 m depth to allow for comparison of soil data across all soils and all corresponding depths. We avoided any soils that showed evidence of colluvial burying (e.g., buried topsoils) or erosion (e.g., missing topsoil or weathered B horizon). We acknowledge that our sampling omits shallower soils on bedrock that can occur at any elevation in our study area, but particularly at higher elevations. The elapsed time since the start of soil formation will undoubtedly vary between sites across our transects given the parent material differences (e.g., Late Quaternary loess, Holocene regolith) and variable erosion rates (and consequently different distributions of soil particle ages). By not selecting very shallow soils, which generally have shorter residence times than deeper soils, we avoid the most extreme temporal inconsistencies. We sampled all soils to 100 cm at 10 cm depth intervals.

Table 1: Overview of the soil sites used in this study.

Site	Latitude (°)	Longitude (°)	NZ Soil classification	Soil Taxonomy	Formation	Elevation (m asl)	Local slope (°)	MAT (°C)	MAP (mm)	PET (mm)
CAMP_01	-43.6238	172.7851	Mottled Fragic Pallic	Fragiudepts	Lyttelton, covered by >1 m loess	83	22	12.3	635	810
CAMP_03	-43.6295	172.7963	Typic Mafic Brown	Dystrudepts	Lyttelton	360	27	11.6	692	769
CAMP_04	-43.6288	172.8002	Typic Mafic Brown	Dystrudepts	Lyttelton	383	9	11.7	694	776
CAMP_06	-43.6342	172.7947	Typic Mafic Melanic	Typic Hapludolls	Mt Herbert	499	19	11.1	767	740
HERB_01	-43.6436	172.7328	Typic Fragic Pallic	Fragiudepts	Stoddart, covered by >1 m loess	272	7	12.2	828	811
HERB_02	-43.6627	172.7355	Typic Mafic Melanic	Typic Hapludolls	Stoddart	493	4	11.0	1266	746
HERB_03	-43.6660	172.7361	Typic Mafic Brown	Dystrudepts	Stoddart	504	7	10.5	1300	717

HERB_04	-43.6614	172.7395	Typic Mafic Brown	Dystrudepts	Stoddart	462	23	11.0	1266	746
LOU_03	-43.6875	172.6929	Typic Mafic Brown	Dystrudepts	Lyttelton	279	20	11.0	1216	760
LOU_05	-43.6909	172.6910	Typic Mafic Melanic	Typic Hapludolls	Lyttelton	288	15	10.6	1214	738
LOU_07	-43.6882	172.7031	Typic Mafic Melanic	Typic Hapludolls	Orton Bradley	490	35	10.4	1240	723

Acid-oxalate extractable Fe, Al, Si (Feo, Alo, Sio) was determined after Blakemore et al. (1987). The acid-oxalate extraction (0.2M oxalate at pH 3; 4 hours shaking in the dark) is used to quantify Fe, Al and Si bound to non-/poorly crystalline secondary soil components, including organic matter-metal complexes. Fe in crystalline pedogenic oxides (Fed) was determined by dithionite-citrate (Blakemore et al., 1987; Holmgren, 1967). Concentrations in the extracts were measured using ICP-OES. Soil pH was determined at a 1:5 soil/water weight ratio after 16h equilibration; electrical conductivity (EC) was also measured at a 1:5 soil:water ratio, shaken for 30 minutes, allowed to settle, and then measured with a temperature-compensated probe (Blakemore et al., 1987). Moisture factor (MF) expresses the difference in moisture between the air-dried sample and the 105°C oven-dried sample (Blakemore et al., 1987). MF has been used as a proxy for reactive surface area (Parfitt et al., 2001). Organic carbon and total nitrogen were analyzed using a LECO TruMac (LECO Corporation, St. Joseph, MO, USA). Phosphate retention (weight %) of the soil was measured after Saunders (1965), using a KH_2PO_4 solution (25 mg P per 5 g of soil). The PO_4 retention of the soil was calculated from the difference between the original P content of the solution and the concentration after shaking the sample for 16 hours. Soil PO_4 retention is an indicator for reactive, pedogenic oxides and metal-organic complexes and usually correlates with acid-oxalate extractions of Fe, Al and Si (Saunders, 1965). Analytic results are reported on 105°C oven-dry basis and represent the <2 mm fraction.

Proximal sensing methods were applied to air-dried samples, ground and passed through a 2 mm sieve. We measured total Ca, Si, K, Ti, Zr, Nb, Al, Fe, and Mn using an Olympus Vanta C series portable XRF (pXRF) instrument (Olympus, Waltham, USA), in bench mode in the laboratory using the internal 'Geochem' element calibration provided by the manufacturer for converting raw spectra into element concentrations as. The instrument is fitted with a Rhodium anode operated at up to 40 KeV with separate beams for light and heavy elements. Prior to analysis, we checked for potential contamination of the pXRF measurement window and tested the instrument measurements against the manufacturer-provided Alloy 316 (stainless steel) calibration check coupon and the NIST standard 2711a. Each sample was measured in a plastic cup, covered by a protective polypropylene 4.0 μm-film. Exposure time was 60 seconds for each beam per sample and measurement uncertainties (1σ) were recorded for each element. Elemental concentrations are reported on 105°C oven-dry basis.

On the same samples we also measured the mid-infrared (MIR) spectra using a Fourier-Transform Infrared (FTIR) spectrophotometer (Tensor II HTS-XT FTIR by Bruker). The spectral range was reduced to the MIR range between 4000 and 600 cm^{-1}. Each sample was scanned in four replicates, then averaged to account for possible heterogeneity within the soil samples. The diffuse reflectance data were transformed into absorbance spectra (absorbance = log [1/reflectance]) prior to statistical analysis.

2.3 Assessment of FTIR data against the altitudinal gradient

Based on previous research (Guillou et al., 2015) we selected a range of wavenumbers of the FTIR data that are particularly indicative of mineralogical differences. We used the following wavenumber regions 3730–3610 cm^{-1}, 1950–1750 cm^{-1}, and 1230–630 cm^{-1} (Guillou et al., 2015). We applied an unconstrained ordination technique (Nonmetric Multidimensional Scaling [NMDS]) to the selected wavenumbers to reduce the dimensions of the multivariate data to two dimensions for visualization and interpretation. The analysis was performed in R version 4.0.2 (R Core Team, 2020) with the 'vegan' package (Oksanen et al., 2019) on untransformed data and with Euclidean distance to calculate the distance matrix of all samples used in the NMDS fitting (Oksanen et al., 2019).

2.4 Parent material modelling using pXRF data

To quantify the proportion of the two parent materials (greywacke loess, volcanics) in each sample, we used the Bayesian mixing model MixSIAR in R (R Core Team, 2020; Stock et al., 2018). In contrast to a simple linear mixing model approach (e.g., $z = f_x b_x + f_y b_y$, $1 = f_x + f_y$; where z is tracer in mixed substrate, b_x is tracer in endmember X, b_y is tracer in endmember Y, f_x and f_y are the relative proportions of the endmembers X and Y), MixSIAR allows us to incorporate the uncertainty derived from endmember variability and random effects (Stock et al., 2018; Stock & Semmens, 2016a, 2016b). We used an uninformative prior and the error structures 'process' and 'residual', which assumes that each sample consists of parent materials that may be derived from different parts of the respective endmember distributions and that the parent materials in each soil can be subject to unknown deviations from the endmember means. As random effect we used the underlying geological formation at each soil site to account for the variability of the volcanic rock geochemistry in our study area. As parent material tracers we chose the ratios of Zr/Ti and Zr/Nb as measured by pXRF in the soils, their suitability as tracers is discussed in detail further below. For the volcanic endmember, we used Zr, Ti and Nb data from Sewell (1988b), as derived from individual samples of the four local geological volcanic rock formations relevant for the individual soil sites (Lyttelton Fm, number of samples (n) = 12; Mt Herbert Fm, n = 11; Orton Bradley Fm, n = 31; Stoddart Fm, n = 26) (Sewell, 1988b; Sewell et al., 1993). To define the loess endmember, we used data from pedogenic C horizons of 4 soils classified as Pallic soils derived from loess, as stored in the New Zealand's National Soil database (soil IDs: SB09997, SB10001, SB10002, SB10004; https://viewer-nsdr.landcareresearch.co.nz/search). In addition, we used data from C horizons of a soil comprising multiple buried loess sheets (Claremont soil; Childs & Searle, 1975). Since the Claremont data set did not contain Nb values, we augmented it with the average of the Nb values from the 4 loess soils in the National Soil Database ($\mu = 12.475$, $\sigma = 1.451$). All of the samples representing loess endmembers come from within 150 km of our study area and received the loess from the same system of braided rivers/alluvial fans as our study area. Total number of endmember loess samples was 24. Three of our soil samples plotted outside the maximum ranges of parent material samples for Zr/Ti or Zr/Nb. These were excluded from the mixing model. Figure S1 shows the endmembers and soil samples in the mixing space. While pXRF data has been previously used for parent material fingerprinting (Mancini et al., 2019), to our knowledge this is the first time that such Bayesian model was used to determine parent material provenance in soils.

245 2.4 Assessment of parent material and climate as soil forming factors using variation
246 partitioning

247 To compare the importance of parent material and climate across our transects in driving
248 the overall variation in the multivariate FTIR dataset, we also performed a variation partitioning
249 using the function *varpart* ('vegan' package). In the variation partitioning we used two sets of
250 explanatory variables: 1) the results of the parent material mixing model for each sample, and 2)
251 a combination of climate parameters for each sample site, where each of the climate parameters
252 (MAT, MAP, PET) interacts with soil depth (i.e., the effects of the parameters change with
253 depth). This approach allows us to partial out the correlation between both factors, parent
254 material and climate (i.e., volcanic rock influence on soils increases with altitude, while at the
255 same time MAT and PET decrease and MAP increases). The FTIR data as the response variable
256 was limited to the upper 50 cm to only include pedogenically altered parts of the soils (i.e., A
257 and B horizons).
258

259 **3 Results**

260 3.1 Soil chemistry and FTIR data of the altitudinal soil gradient

261 Most chemical soil properties (e.g., moisture factor, organic C, PO_4^- retention, various
262 fractions of Fe and Al, most of the total elements) confirm the intermediate chemical character of
263 Brown soils between Pallic and Melanic soils (Figure 2). Some variables show a particularly
264 strong contrast between soils derived from loess and volcanic parent material as represented by
265 Pallic and Melanic soils: higher concentrations of Fe, Al, Mn and Ti occur in Melanic soils,
266 whereas Si and K show higher concentrations in Pallic soils. Melanic soils show a characteristic
267 increase in K concentrations of K towards the surface. Ca concentrations in Melanic soils are, on
268 average, indifferent to those of Pallic or Brown soils. Soil pH values are on average slightly
269 lower in Melanic soils. Crystalline and non-crystalline pedogenic oxides, organic carbon and
270 moisture factor are lowest in Pallic soils and increase towards Brown and Melanic soils.

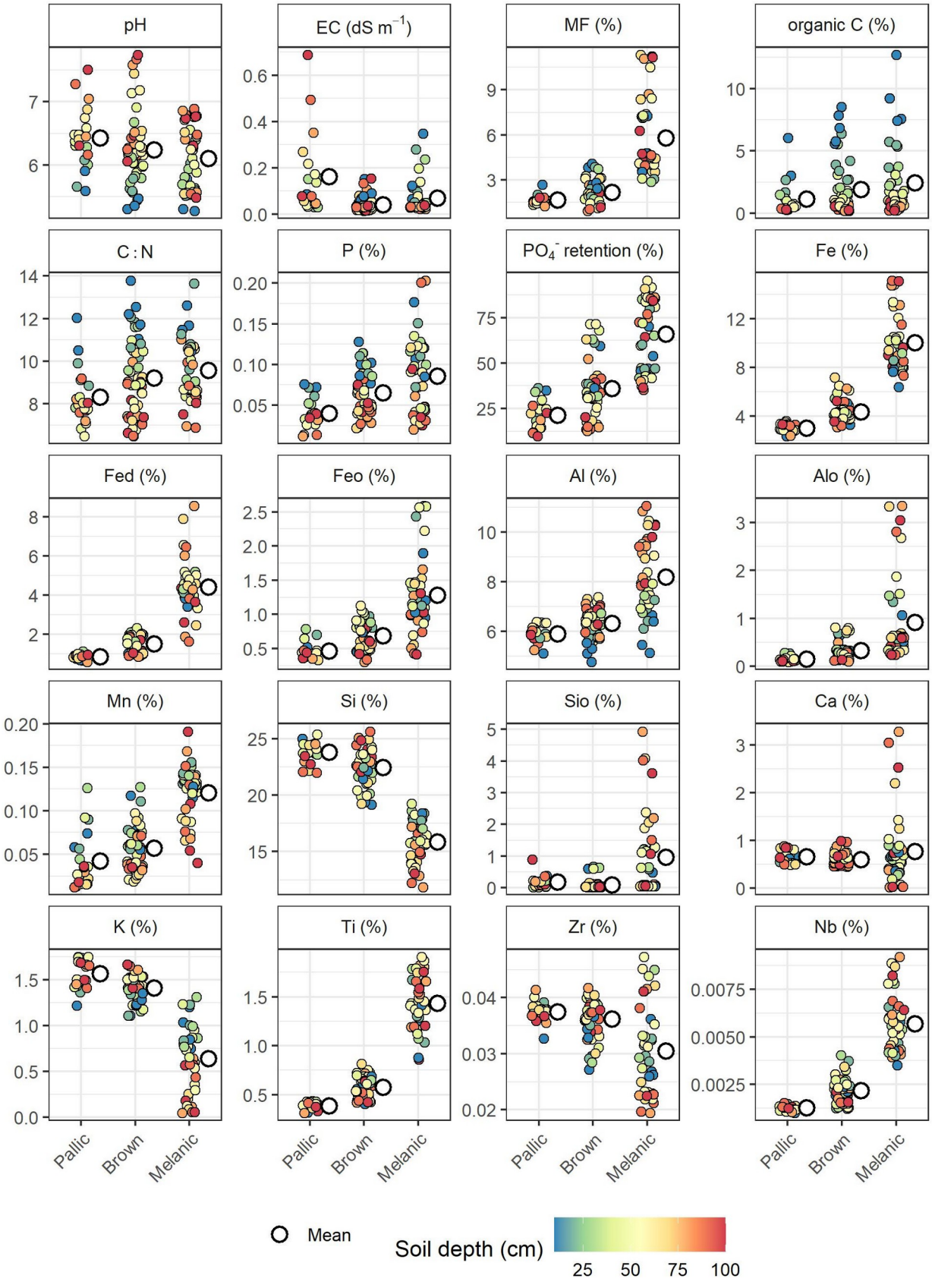
pH
EC (dS m^{-1})
MF (%)
organic C (%)
C : N
P (%)
PO_4^- retention (%)
Fe (%)
Fed (%)
Feo (%)
Al (%)
Alo (%)
Mn (%)
Si (%)
Sio (%)
Ca (%)
K (%)
Ti (%)
Zr (%)
Nb (%)
Pallic
Brown
Melanic
Mean
Soil depth (cm)
25
50
75
100

271

Figure 2: Summary of the selected soil chemical properties. The data is summarised by the mean of each soil order, offset to the right of the raw data.

The FTIR data in ordination space across the three main soils show a general drift across the x-axis values (NMDS1), in the order of Pallic soils < Brown soils < Melanic soils (Figure 3). Towards the surface, Melanic soils show smaller x-axis values, whereas the opposite but less clear trend seems to apply to Pallic and Brown soils. Overall, this results in an increasing convergence of the three soil orders towards the center of the ordination as soil depth becomes shallower. This increasing similarity of shallow samples is also corroborated by the chemistry data that shows lower absolute differences between the three soil orders as depth becomes shallower, particularly for the Melanic – Pallic/Brown comparison (Figure 2). Across both ordination axes Melanic soils show the largest variation compared to Pallic and Brown soils (Figure 3), a pattern that is also reflected in the variability of chemical properties, including those of our tracer elements (Ti, Zr, Nb) (Figure 2).

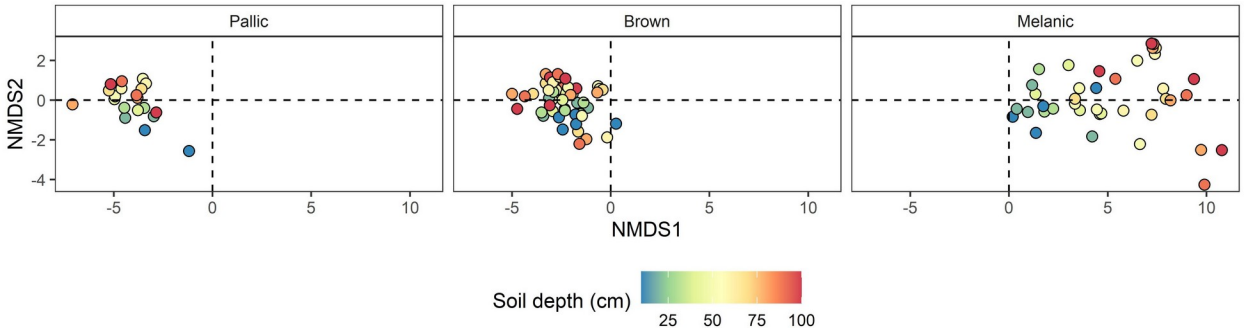

Figure 3: NMDS ordination of the selected FTIR wavenumbers with indication of soil depth (base of sample), by soil order. Each soil order was plotted separately for better readability; the ordination space for all three panels is identical.

3.2 Parent material modelling

The Bayesian mixing model results agree with the expected dominance of loess parent material in Pallic soils and that of volcanics in Melanic soils. Figure 4 shows the proportions of volcanic parent material across the depths of the soils. While the 95% confidence intervals are generally larger for Brown soils, these soils still form a distinct group in between the two endmember soil groups. In the soils CAMP_03 and 04, volcanic-dominated substrate is placed over more loess-dominated material, while the opposite case is indicated for HERB_04, and an even more complex deposition history is recorded for HERB_03. In contrast, LOU_03 shows a more monotonous depth relationship of the volcanic contribution.

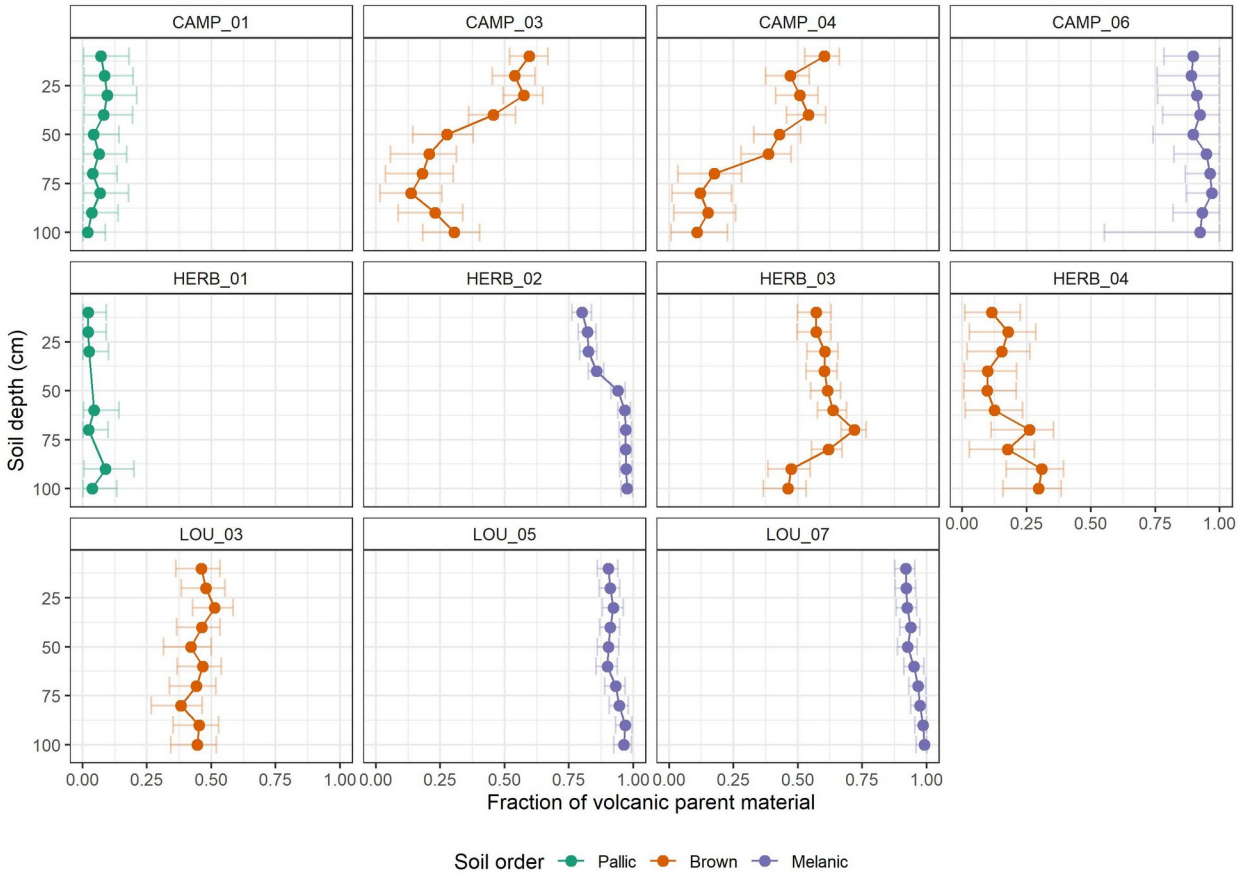

Figure 4: Mixing proportions with soil depth. Shown are medians and 95% confidence intervals of the fractions of volcanic parent material contribution to each depth increment.

3.3 Parent material and climate as soil forming factors

The results of the variation partitioning (Figure S2) show that parent material alone accounts for 31% of the variation in the FTIR data, equal to the shared amount explained by parent material and climate. The shared amount reflects the spatial correlation of parent material and climate across our gradient. Only 9% of variation could be assigned to climate alone, while 29% of total variation is explained by unknown variables (residuals). Without partitioning out the correlation between climate and parent material, climate would account for almost 40% of the total variation, whereas parent material would reach 62%.

4 Discussion

Through a combination of soil spectral data, Bayesian mixing modelling and multivariate statistics we were able to quantify the effect of the two spatially correlated soil forming factors, parent material and climate, on soil formation. Our results indicate the dominance of parent material over climate as controlling factor in soil formation across our altitudinal gradient.

4.1 Confirmation of the existing soil-landscape relationship

Initially we confirmed the consistency of the soil chemical and spectral data with the observed soil morphology and classification that formed the basis for the existing soil-landscape

model. The soil data confirms the intermediate chemical character of Brown soils between the loess-derived, low elevation Pallic and volcanics-derived, high elevation Melanic soils (Figures 2 and 3). This is consistent with the existing understanding that the Brown soil characteristics are both the result of parent material mixing (loess, volcanics) and mid-elevation climate. The particularly strong contrast between soils derived from loess (Pallic) and volcanic parent material (Melanic) in many elements reflects the strong imprint of mineralogy. Olivine, pyroxene, and Fe-Ti oxides (and their weathering products) as typical minerals in the volcanic rock result in the high concentrations of Fe, Al, Mn and Ti in Melanic, whereas the quartz and K-feldspar components of in loess are behind the high Si and K concentrations in Pallic soils. The increasing concentrations of K towards the surface in Melanic soils is likely indicative of plant uplift (Jobbagy & Jackson, 2004) resulting in similar topsoil values across all soils despite the differences of K concentrations in the parent material. The overall increasing similarity of the shallow soil increments in all soils as indicated but the ordination of the FTIR data (Figure 3) is likely a consequence of the similar pastoral land use across all sites. Albeit not directly measured by us, from the mineral assemblage and the large Fe concentrations we would also expect to see a much larger concentration of Mg as derived from olivine in Melanic soils. Surprisingly, Ca concentrations are on average indifferent between soil orders. This may indicate that the general higher abundance of Ca-rich plagioclase feldspars in volcanic parent material as compared to albite/orthoclase-rich loess is not replicated in our soils despite Ca-rich plagioclase being consistently listed as the main mineral of the local volcanic rocks in the extensive dataset ($n > 200$) by Sewell (1988b). Therefore, we think it is more likely that higher weathering and leaching rates of base metals under a wetter climate at higher elevations has depleted Ca in most Melanic soils. This is supported by the lower soil pH values in Melanic soils, which indicates that the increased proton-supply driven by higher precipitation has more than compensated for the initially larger buffer capacity derived from basic volcanic parent material in Melanic soils in comparison to more felsic but drier loess soils. In addition, weathering rates of Ca- and Mg-rich feldspars and other silicates found in volcanic parent material are higher than those of Na- or K-feldspars and quartz that dominate the loess mineralogy given their higher solubility constants (e.g., thermodynamic databases used by gechemical transport models; Parkhurst & Appelo, 2013; Steefel et al., 2015). Similarly, higher concentrations of crystalline and non-crystalline pedogenic oxides in Melanic soils is likely to be a result of a wetter climate but also more easily weatherable primary minerals releasing Fe, Al, and Si at higher rates, even despite total Si content is much lower in Melanic soils. Given that organic carbon and moisture factor are tightly linked to pedogenic oxides (e.g., Kirsten et al., 2021; Kleber et al., 2005; McNally et al., 2017; Mikutta et al., 2006; Wiesmeier et al., 2019), their concomitant increase in Melanic soils is unsurprising. Overall, we interpret the increased variability in in chemical properties and FTIR ordination in Melanic soils (Figures 2 and 3) as an indicator for more advanced pedogenic alterations than in the other soil orders, including secondary mineral formation (e.g., pedogenic oxides), organic matter accumulation, and weathering and leaching (e.g., dilution/residual enrichment of chemical index elements), causing increased horizontal differentiation within the Melanic soils as a combination of higher mineral weathering rates and a wetter climate at higher altitude.

In summary, the combined chemical and spectral datasets are consistent with expected climate and parent material changes originally based on qualitative, soil morphological assessments. To disentangle the contribution of climate and parent material as a control of this pattern, we quantified the parent material contribution to each sample.

4.2 Soil parent material modelling using immobile elements and Bayesian mixing model

Before performing the mixing model we evaluated the assumption that Zr, Ti and Nb are appropriate tracers for parent material. Zr, Ti and Nb are all elements that show minimal chemical reactivity and mobility in soils because of low solubility (valence states of +4 and +5). They have been widely used in pedology and geochemistry as conservative tracer for quantitative mass balance calculations and geochemical source partitioning (e.g., Brantley & White, 2009; O. A. Chadwick et al., 1990; O. A. Chadwick et al., 1999; Egli & Fitze, 2000; Ferrier et al., 2011; Muhs et al., 2010; Riebe et al., 2003; White et al., 1998; Yoo et al., 2007). We assume that the ratios of these elements in our soils only change due to parent material changes but are irresponsive to chemical weathering. This is a simplification since variability within a parent material group, and unknown external inputs to the soil can also affect these ratios (e.g., Kurtz et al., 2000; Oeser et al., 2018). In addition, there is evidence that even low-solubility elements can get mobilized under certain conditions (e.g., Cornu et al., 1999; Du et al., 2012; Hodson, 2002). To test for immobility in natural conditions, the suspected immobile elements are usually compared with each other to identify the most residually enriched elements in the most chemically altered samples (e.g., Kurtz et al., 2000; Oeser et al., 2018). However, this is not definitive evidence that an identified most enriched element is indeed immobile, rather that it may be the least mobile elements out of all measured elements.

Figure S3 shows Zr plotted against Ti and Nb in each soil with depth. Even Pallic and Melanic soils that we initially assumed to be either derived from loess or volcanic parent material, respectively, show some variability. The data from HERB_02 even indicates that compared to Zr, Nb and Ti are increasingly leached from the upper 40 cm of the profile. However, we have confidence in using the selected element ratios as tracers in our mixing model for two reasons. Firstly, within the context of the complete mixing space of soils and parent material endmembers (Figure S1), the variability of the ratios of immobile elements in Pallic and Melanic soils has limited impact. The variability in the Pallic soils is entirely contained within the ranges of Zr/Nb, and Zr/Ti in the endmember samples of the loess. For the Melanic soils, samples are mostly contained within the linear mixing space and, while a preferential leaching of Nb and Ti compared to Zr could be behind the shift of some samples of Melanic soils beneath the linear relationship, potentially overestimating the loess component in soils by interpreting larger Zr/Ti and Zr/Nb ratios due to weathering as parent material signals instead. The alternative explanation would be that even soils that we assume to be derived from volcanic parent material still have a low loess input (e.g., HERB_02). Secondly, Figure S1 shows that the variability of immobile element ratios within each parent material endmember is small in comparison to the differences between the loess and volcanics. In addition, Figure S1 indicates that there is little evidence for an additional parent material endmember in the soils, given the near-linear relationship between endmembers and soil samples.

The results of the mixing model confirm the expected dominance of loess parent material in Pallic soils, that of volcanics in Melanic soils and the mixed parent material in Brown soils (Figure 4). Overall, the results of the mixing model are consistent with other indicators of parent material provenance with minor modification by climate (Figure 5): total Si content decreases with increasing proportion of volcanics in each sample as loess-derived quartz content declines. The opposite pattern applies to total Fe as Fe-bearing minerals increase with increased volcanic input. Concerning more mobile base metals, total K content decreases with increasing proportion of volcanics as loess-derived K-feldspar content declines but likely also due to increased

leaching in volcanic-dominated soils limited to higher altitudes under greater precipitation. Increased leaching at higher altitude is also likely behind the lack of a correlation of total Ca with parent material provenance effectively offsetting the larger Ca content of unweathered volcanic parent material, except for deeper subsoil increments as discussed above. While an overestimation of the loess parent material may occur in our model, the effect appears to be limited given the consistent relationships with the chemical proxies. HERB_02, which showed the strongest indication that Ti and Nb is mobilized in the soil compared to Zr (Figure S3), is still overwhelmingly dominated by volcanic parent material.

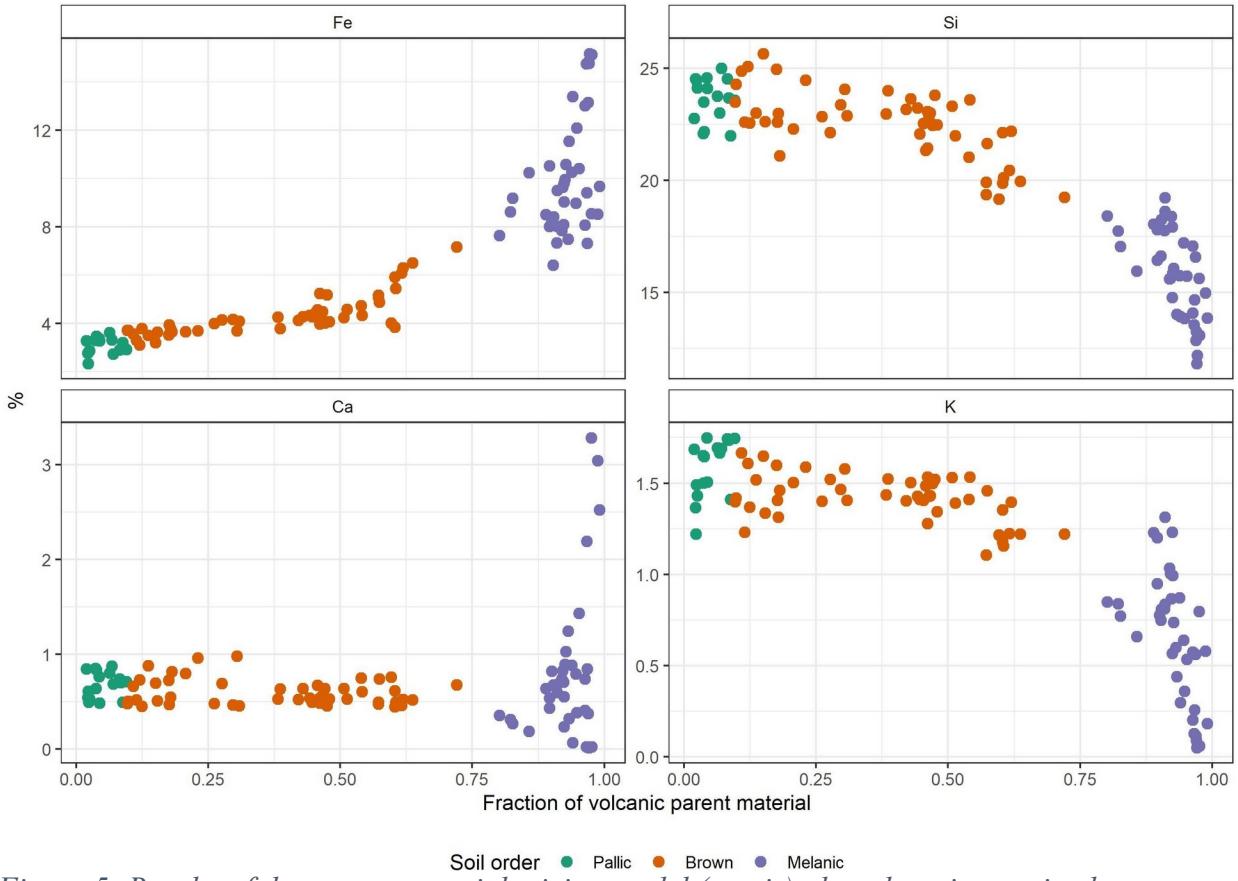

Figure 5: Results of the parent material mixing model (x-axis) plotted against main element concentrations (y-axis). Note the panel headings for the different elements. Modelled parent material proportions of the volcanic rock (1-x for loess) grouped by soil order are consistent with mineralogy and climate.

4.3 Importance of parent material and climate as soil forming factors

The results from the variation partitioning indicate that parent material explains a much larger variation in the FTIR data than climate. Given the distinct mineralogical differences between felsic greywacke loess and mafic volcanics, this result is plausible. However, our observations have practical relevance for digital soil mapping. Many digital soil mapping approaches focus on quantitative, spatial covariates. Across the set of soil forming factors, climate, vegetation and topography are generally available in this quantitative form, given the

advances in digital elevation models, lidar, remote sensing, and spatial modelling of climate parameters. In contrast, spatial information on parent material is mostly available only as categorical variables (e.g., lithology classes of geological maps), or do not exist at the required mapping scales. Therefore, it is unsurprising that parent material has often been omitted in the sets of covariates used for digital soil mapping (Gray et al., 2016; Grunwald, 2009; Lamichhane et al., 2019). In our case study, if we only used climate parameters to explain the FTIR data, we would 1) potentially misidentify climate as the major driver of variability across our altitude gradient and miss the significance of parent material for the soils, and 2) loose the large explanatory power of parent material in modelling/predicting the soil properties data.

Our example emphasizes the relevance of parent material characterization for explaining soil properties in a landscape context. Our results suggest that a consideration of parent material can not only aid the predictive capability of statistical and otherwise models, but also enhance the utility of such models for understanding the mechanistic drivers of soil properties within a spatial context (see also Gray et al., 2016). We therefore advocate for more efforts towards developing quantitative soil parent material data sets adequate for the scale and environmental conditions of the mapping space, and encourage their use in digital soil mapping (e.g., Bonfatti et al., 2020; Gray et al., 2016; Mancini et al., 2019).

5 Conclusions

We used an altitudinal soil gradient with concomitant changes of greywacke loess to volcanic rock, and drier to wetter climate, to show how relatively inexpensive and rapid soil spectral methods can help to the separate the effects of parent material and climate in driving soil properties. We used chemically conservative tracer elements combined with a Bayesian mixing model to identify the parent material contribution in each sample and found that the results were consistent with other soil chemical data. By partitioning out the spatial correlation between climate and parent material using a variation analysis, we were able to statistically confirm that parent material and not climate explains a larger part of the variation in our FTIR soil spectra. We conclude that multivariate statistics, and mixing models coupled to soil spectroscopy are useful tools to improve our understanding of landscape-scale drivers of soil variation even when multiple factors change concomitantly. Our work emphasizes the role of parent material as an important explanatory, but often neglected, variable in modern soil mapping.

Acknowledgments, Samples, and Data

The raw data for this publication and R code used in the data analyses are available in the supplementary material and under https://datastore.landcareresearch.co.nz/dataset/jgr-soilformingfactors. We thank the landowners for access to the sampling sites. The work was partially funded by the Ministry of Business and Innovation through the Strategic Science Investment Fund to Manaaki Whenua-Landcare Research (MWLR). The conception of the work benefitted from a soil survey contract awarded to MWLR by Environment Canterbury and unpublished reports by B. B. Trangmar and J. S. Whitton of the former NZ Soil Bureau. We thank Ngaire Forster and her staff at MWLR's soil chemistry laboratory for the soil analysis, Hugh Smith and Pierre Roudier for discussions of some aspects of this work, and Yuxin Ma for reviewing an earlier version of this work.

References

Agbenin, J. O., & Tiessen, H. (1994). Phosphorus transformations in a toposequence of lithosols and cambisols from semi-arid northeastern brazil. *Geoderma, 62*(4), 345-362. http://www.sciencedirect.com/science/article/pii/0016706194900981

Araújo, M. S. B., Schaefer, C. E. R., & Sampaio, E. V. S. B. (2004). Soil phosphorus fractions from toposequences of semi-arid Latosols and Luvisols in northeastern Brazil. *Geoderma, 119*(3–4), 309-321. http://www.sciencedirect.com/science/article/pii/S0016706103002702

Bazilevskaya, E., Lebedeva, M., Pavich, M., Rother, G., Parkinson, D. Y., Cole, D., & Brantley, S. L. (2013). Where fast weathering creates thin regolith and slow weathering creates thick regolith. *Earth Surface Processes and Landforms, 38*(8), 847-858. https://onlinelibrary.wiley.com/doi/abs/10.1002/esp.3369

Behrens, T., & Viscarra Rossel, R. A. (2020). On the interpretability of predictors in spatial data science: the information horizon. *Scientific Reports, 10*(1), 16737. https://doi.org/10.1038/s41598-020-73773-y

Blakemore, L. C., Searle, B. K., & Daly, B. K. N. (1987). Methods for chemical analysis of soils. *Soil Bureau Scientific Report, 80*.

Bonfatti, B. R., Demattê, J. A. M., Marques, K. P. P., Poppiel, R. R., Rizzo, R., Mendes, W. d. S., et al. (2020). Digital mapping of soil parent material in a heterogeneous tropical area. *Geomorphology, 367*, 107305. https://www.sciencedirect.com/science/article/pii/S0169555X20302774

Brantley, S. L., & White, A. F. (2009). Approaches to Modeling Weathered Regolith. *Reviews in Mineralogy and Geochemistry, 70*(1), 435-484. https://doi.org/10.2138/rmg.2009.70.10

Chadwick, K. D., & Asner, G. P. (2020). Geomorphic transience moderates topographic controls on tropical canopy foliar traits. *Ecology Letters, 23*(8), 1276-1286. https://onlinelibrary.wiley.com/doi/abs/10.1111/ele.13531

Chadwick, O. A., Brimhall, G. H., & Hendricks, D. M. (1990). From a black to a gray box -- a mass balance interpretation of pedogenesis. *Geomorphology, 3*(3-4), 369-390.

Chadwick, O. A., Derry, L., Vitousek, P., Huebert, B., & Hedin, L. (1999). Changing sources of nutrients during four million years of ecosystem development. *Nature, 397*(6719), 491-497.

Chadwick, O. A., Gavenda, R. T., Kelly, E. F., Ziegler, K., Olson, C. G., Elliott, W. C., & Hendricks, D. M. (2003). The impact of climate on the biogeochemical functioning of volcanic soils. *Chemical Geology, 202*(3-4), 195-223.

Childs, C. W., & Searle, P. L. (1975). *Element distributions in loess columns at Claremont, Table Flat and Stewarts Claim, New Zealand*. Retrieved from http://doi.org/10.7931/DL1-SBSR-20

Cornu, S., Lucas, Y., Lebon, E., Ambrosi, J. P., Luizão, F., Rouiller, J., et al. (1999). Evidence of titanium mobility in soil profiles, Manaus, central Amazonia. *Geoderma, 91*(3-4), 281-295.

Crews, T. E., Kitayama, K., Fownes, J. H., Riley, R. H., Herbert, D. A., Mueller-Dombois, D., & Vitousek, P. M. (1995). Changes in Soil Phosphorus Fractions and Ecosystem Dynamics across a Long Chronosequence in Hawaii. *Ecology, 76*(5), 1407-1424.

Dere, A. L., White, T. S., April, R. H., Reynolds, B., Miller, T. E., Knapp, E. P., et al. (2013). Climate dependence of feldspar weathering in shale soils along a latitudinal gradient. *Geochimica et Cosmochimica Acta, 122*, 101-126. https://doi.org/10.1016/j.gca.2013.08.001

Dixon, J. L., Chadwick, O. A., & Vitousek, P. M. (2016). Climate-driven thresholds for chemical weathering in postglacial soils of New Zealand. *Journal of Geophysical Research: Earth Surface, 121*(9), 1619-1634. https://agupubs.onlinelibrary.wiley.com/doi/abs/10.1002/2016JF003864

Dorji, T., Caspari, T., Bäumler, R., Veldkamp, A., Jongmans, A., Tshering, K., et al. (2009). Soil development on Late Quaternary river terraces in a high montane valley in Bhutan, Eastern Himalayas. *CATENA, 78*(1), 48-59.

Du, X., Rate, A. W., & Gee, M. A. M. (2012). Redistribution and mobilization of titanium, zirconium and thorium in an intensely weathered lateritic profile in Western Australia. *Chemical Geology, 330-331*, 101-115. http://www.sciencedirect.com/science/article/pii/S0009254112003890

Eger, A., Almond, P. C., & Condron, L. M. (2011). Pedogenesis, soil mass balance, phosphorus dynamics and vegetation communities across a Holocene soil chronosequence in a super-humid climate, South Westland, New Zealand. *Geoderma, 163*(3-4), 185-196. http://www.sciencedirect.com/science/article/pii/S0016706111000875

Egli, M., & Fitze, P. (2000). Formulation of pedologic mass balance based on immobile elements: a revision. *Soil Science, 165*(5), 437-443.

Ferrier, K. L., Kirchner, J. W., & Finkel, R. C. (2011). Estimating millennial-scale rates of dust incorporation into eroding hillslope regolith using cosmogenic nuclides and immobile weathering tracers. *J. Geophys. Res., 116*(F3), F03022. http://dx.doi.org/10.1029/2011JF001991

Gray, J. M., Bishop, T. F. A., & Wilford, J. R. (2016). Lithology and soil relationships for soil modelling and mapping. *CATENA, 147*, 429-440. https://www.sciencedirect.com/science/article/pii/S0341816216303046

Griffiths, E. (1973). Loess of Banks Peninsula. *New Zealand Journal of Geology and Geophysics, 16*(3), 657-675. https://doi.org/10.1080/00288306.1973.10431388

Grunwald, S. (2009). Multi-criteria characterization of recent digital soil mapping and modeling approaches. *Geoderma, 152*(3), 195-207. https://www.sciencedirect.com/science/article/pii/S0016706109001827

Guillou, F. L., Wetterlind, W., Viscarra Rossel, R. A., Hicks, W., Grundy, M., & Tuomi, S. (2015). How does grinding affect the mid-infrared spectra of soil and their multivariate calibrations to texture and organic carbon? *Soil Research, 53*(8), 913-921. https://www.publish.csiro.au/paper/SR15019

Hahm, W. J., Riebe, C. S., Lukens, C. E., & Araki, S. (2014). Bedrock composition regulates mountain ecosystems and landscape evolution. *Proceedings of the National Academy of Sciences, 111*(9), 3338-3343. http://www.pnas.org/content/111/9/3338.abstract

Helfenstein, J., Tamburini, F., von Sperber, C., Massey, M. S., Pistocchi, C., Chadwick, O. A., et al. (2018). Combining spectroscopic and isotopic techniques gives a dynamic view of phosphorus cycling in soil. *Nature Communications, 9*(1), 3226. https://doi.org/10.1038/s41467-018-05731-2

Heung, B., Ho, H. C., Zhang, J., Knudby, A., Bulmer, C. E., & Schmidt, M. G. (2016). An overview and comparison of machine-learning techniques for classification purposes in digital soil mapping. *Geoderma, 265*, 62-77. https://www.sciencedirect.com/science/article/pii/S0016706115301300

Hewitt, A. E. (1993). New Zealand soil classification. *Landcare Research science series, 1*, 1-133.

Hodson, M. E. (2002). Experimental evidence for mobility of Zr and other trace elements in soils. *Geochimica et Cosmochimica Acta, 66*(5), 819-828.

Holmgren, G. G. S. (1967). A Rapid Citrate-Dithionite Extractable Iron Procedure. *Soil Science Society of America Journal, 31*(2), 210-211. https://acsess.onlinelibrary.wiley.com/doi/abs/10.2136/sssaj1967.03615995003100020020x

Jenny, H. (1941). *Factors of soil formation: a system of quantitative pedology*. New York: Mc-Graw-Hill.

Jobbagy, E. G., & Jackson, R. B. (2004). The uplift of soil nutrients by plants: biogeochemical consequences across scales. *Ecology, 85*(9), 2380-2389. http://www.esajournals.org/doi/abs/10.1890/03-0245

Jowett, T. W. D. (1995). *An Investigation of the Geotechnical properties of loess from Canterbury and Marlborough.* (MSc), University of Canterbury, Christchurch.

Kirsten, M., Mikutta, R., Vogel, C., Thompson, A., Mueller, C. W., Kimaro, D. N., et al. (2021). Iron oxides and aluminous clays selectively control soil carbon storage and stability in the humid tropics. *Scientific Reports, 11*(1), 5076. https://doi.org/10.1038/s41598-021-84777-7

Kleber, M., Mikutta, R., Torn, M. S., & Jahn, R. (2005). Poorly crystalline mineral phases protect organic matter in acid subsoil horizons. *European Journal of Soil Science, 56*(6), 717-725. http://dx.doi.org/10.1111/j.1365-2389.2005.00706.x

Kurtz, A. C., Derry, L. A., Chadwick, O. A., & Alfano, M. J. (2000). Refractory element mobility in volcanic soils. *Geology, 28*(8), 683-686. http://geology.geoscienceworld.org/cgi/content/abstract/28/8/683

Lamichhane, S., Kumar, L., & Wilson, B. (2019). Digital soil mapping algorithms and covariates for soil organic carbon mapping and their implications: A review. *Geoderma, 352*, 395-413. https://www.sciencedirect.com/science/article/pii/S0016706119300540

Leathwick, J. R., New Zealand. Ministry for the, E., Manaaki Whenua-Landcare Research New Zealand, L., & Landcare Research New, Z. (2002). *Land environments of New Zealand = Nga taiao o Aotearoa : a technical guide*. Auckland: Ministry for the Environment.

Leslie, D. M. (1973a). Quaternary deposits and surfaces in a volcanic landscape on Otago Peninsula. *New Zealand Journal of Geology and Geophysics, 16*(3), 557-566. https://doi.org/10.1080/00288306.1973.10431378

Leslie, D. M. (1973b). Relationship between soils and regolith in a volcanic landscape on Otago Peninsula. *New Zealand Journal of Geology and Geophysics, 16*(3), 567-574. https://doi.org/10.1080/00288306.1973.10431379

Ma, Y., Minasny, B., & Wu, C. (2017). Mapping key soil properties to support agricultural production in Eastern China. *Geoderma Regional, 10*, 144-153. https://www.sciencedirect.com/science/article/pii/S2352009417300615

Mage, S. M., & Porder, S. (2013). Parent Material and Topography Determine Soil Phosphorus Status in the Luquillo Mountains of Puerto Rico. *Ecosystems, 16*(2), 284-294. journal article. http://dx.doi.org/10.1007/s10021-012-9612-5

Maher, K., Steefel, C. I., White, A. F., & Stonestrom, D. A. (2009). The role of reaction affinity and secondary minerals in regulating chemical weathering rates at the Santa Cruz Soil Chronosequence, California. *Geochimica et Cosmochimica Acta, 73*(10), 2804-2831. http://www.sciencedirect.com/science/article/pii/S0016703709000775

Manaaki Whenua - Landcare Research. (2020). *S-map - New Zealand's national digital soil map*. Retrieved from: doi.org/10.7931/L1WC7

Mancini, M., Weindorf, D. C., Chakraborty, S., Silva, S. H. G., dos Santos Teixeira, A. F., Guilherme, L. R. G., & Curi, N. (2019). Tracing tropical soil parent material analysis via portable X-ray fluorescence (pXRF) spectrometry in Brazilian Cerrado. *Geoderma, 337*, 718-728. https://www.sciencedirect.com/science/article/pii/S0016706118316069

McBratney, A. B., Mendonça Santos, M. L., & Minasny, B. (2003). On digital soil mapping. *Geoderma, 117*(1), 3-52. https://www.sciencedirect.com/science/article/pii/S0016706103002234

McNally, S. R., Beare, M. H., Curtin, D., Meenken, E. D., Kelliher, F. M., Calvelo Pereira, R., et al. (2017). Soil carbon sequestration potential of permanent pasture and continuous cropping soils in New Zealand. *Global Change Biology, 23*(11), 4544-4555. https://onlinelibrary.wiley.com/doi/abs/10.1111/gcb.13720

Meyer, H., Reudenbach, C., Wöllauer, S., & Nauss, T. (2019). Importance of spatial predictor variable selection in machine learning applications – Moving from data reproduction to spatial prediction. *Ecological Modelling, 411*, 108815. https://www.sciencedirect.com/science/article/pii/S0304380019303230

Mikutta, R., Kleber, M., Torn, M. S., & Jahn, R. (2006). Stabilization of Soil Organic Matter: Association with Minerals or Chemical Recalcitrance? *Biogeochemistry, 77*(1), 25-56. https://doi.org/10.1007/s10533-005-0712-6

Ministry for the Environment. (2002). LENZ - Annual water deficit (Publication no. https://doi.org/10.7931/L1KM2). from Ministry for the Environment

Muhs, D. R., Budahn, J., Avila, A., Skipp, G., Freeman, J., & Patterson, D. (2010). The role of African dust in the formation of Quaternary soils on Mallorca, Spain and implications for the genesis of Red Mediterranean soils. *Quaternary Science Reviews, 29*(19), 2518-2543. http://www.sciencedirect.com/science/article/pii/S0277379110001228

Odgers, N. P., McBratney, A. B., & Minasny, B. (2011). Bottom-up digital soil mapping. II. Soil series classes. *Geoderma, 163*(1), 30-37. https://www.sciencedirect.com/science/article/pii/S0016706111000760

Oeser, R. A., Stroncik, N., Moskwa, L.-M., Bernhard, N., Schaller, M., Canessa, R., et al. (2018). Chemistry and microbiology of the Critical Zone along a steep climate and vegetation gradient in the Chilean Coastal Cordillera. *CATENA, 170*, 183-203. http://www.sciencedirect.com/science/article/pii/S034181621830225X

Oksanen, J., Blanchet, F. G., Friendly, M., Kindt, R., Legendre, P., McGlinn, D., et al. (2019). vegan: Community Ecology Package (Version R package version 2.5-6). Retrieved from https://CRAN.R-project.org/package=vegan

Parfitt, R. L., Whitton, J. S., & Theng, B. K. G. (2001). Surface reactivity of A horizons towards polar compounds estimated from water adsorption and water content. *Soil Research, 39*(5), 1105-1110. https://www.publish.csiro.au/paper/SR00059

Parkhurst, D. L., & Appelo, C. A. J. (2013). *Description of input and examples for PHREEQC version 3 - A computer program for speciation, batch-reaction, one-dimensional transport, and inverse geochemical calculations*. Denver: U.S. Geological Survey.

Porder, S., Paytan, A., & Vitousek, P. M. (2005). Erosion and landscape development affect plant nutrient status in the Hawaiian Islands. *Oecologia, 142*(3), 440-449. https://doi.org/10.1007/s00442-004-1743-8

R Core Team. (2020). R: A language and environment for statistical computing. Vienna: R Foundation for Statistical Computing. Retrieved from https://www.R-project.org/

Raeside, J. D. (1964). Loess Deposits of the South Island, New Zealand, and Soils Formed on them. *New Zealand Journal of Geology and Geophysics, 7*(4), 811-838. https://doi.org/10.1080/00288306.1964.10428132

Richardson, S. J., Allen, R. B., & Doherty, J. E. (2008). Shifts in leaf N:P ratio during resorption reflect soil P in temperate rainforest. *Functional Ecology, 22*(4), 738-745. http://dx.doi.org/10.1111/j.1365-2435.2008.01426.x

Richardson, S. J., Peltzer, D. A., Allen, R. B., McGlone, M. S., & Parfitt, R. L. (2004). Rapid development of phosphorus limitation in temperate rainforest along the Franz Josef soil chronosequence. *Oecologia, 139*(2), 267-276. https://doi.org/10.1007/s00442-004-1501-y

Riebe, C. S., Kirchner, J. W., & Finkel, R. C. (2003). Long-term rates of chemical weathering and physical erosion from cosmogenic nuclides and geochemical mass balance. *Geochimica et Cosmochimica Acta, 67*(22), 4411-4427.

Riebe, C. S., Kirchner, J. W., & Finkel, R. C. (2004). Erosional and climatic effects on long-term chemical weathering rates in granitic landscapes spanning diverse climate regimes. *Earth and Planetary Science Letters, 224*(3-4), 547-562. https://doi.org/10.1016/j.epsl.2004.05.019

Saunders, W. M. H. (1965). Phosphate retention by New Zealand soils and its relationship to free sesquioxides, organic matter, and other soil properties. *New Zealand Journal of Agricultural Research, 8*(1), 30-57. https://doi.org/10.1080/00288233.1965.10420021

Sewell, R. J. (1988a). Late Miocene volcanic stratigraphy of central Banks Peninsula, Canterbury, New Zealand. *New Zealand Journal of Geology and Geophysics, 31*(1), 41-64. https://doi.org/10.1080/00288306.1988.10417809

Sewell, R. J. (1988b). *The volcanic geology and geochemistry of central Banks Peninsula and relationships to Lyttelton and Akaroa volcanoes.* (PhD), University of Canterbury, Christchurch.

Sewell, R. J., Reay, M. B., & Mercury, W. (1993). *Geology of Banks Peninsula. Scale 1:100 000*. Lower Hutt, N.Z.: Institute of Geological and Nuclear Sciences.

Soil Survey Staff. (1999). *Soil taxonomy* (2nd ed. Vol. 436): United States Department of Acriculture.

Steefel, C. I., Appelo, C. A. J., Arora, B., Jacques, D., Kalbacher, T., Kolditz, O., et al. (2015). Reactive transport codes for subsurface environmental simulation. *Computational Geosciences, 19*(3), 445-478.

Stock, B. C., Jackson, A. L., Ward, E. J., Parnell, A. C., Phillips, D. L., & Semmens, B. X. (2018). Analyzing mixing systems using a new generation of Bayesian tracer mixing models. *PeerJ, 6*, e5096

Stock, B. C., & Semmens, B. X. (2016a). *MixSIAR GUI User Manual*. In. Retrieved from https://github.com/brianstock/MixSIAR/ doi:10.5281/zenodo.47719

Stock, B. C., & Semmens, B. X. (2016b). Unifying error structures in commonly used biotracer mixing models. *Ecology, 97*(10), 2562-2569. https://esajournals.onlinelibrary.wiley.com/doi/abs/10.1002/ecy.1517

Tonkin, P. J., & Basher, L. R. (2001). Soil chronosequences in subalpine superhumid Cropp Basin, western Southern Alps, New Zealand. *New Zealand Journal of Geology & Geophysics, 44*, 37-45.

Trangmar, B. B. (1986). *Soil-landscape relationships Barrys Bay-Wainui District, Banks Peninsula*. Retrieved from http://doi.org/10.7931/DL1-DOR-CH20

Turner, B. L., Hayes, P. E., & Laliberté, E. (2018). A climosequence of chronosequences in southwestern Australia. *European Journal of Soil Science, 69*(1), 69-85. https://onlinelibrary.wiley.com/doi/abs/10.1111/ejss.12507

Turner, S., Mikutta, R., Meyer-Stüve, S., Guggenberger, G., Schaarschmidt, F., Lazar, C. S., et al. (2017). Microbial Community Dynamics in Soil Depth Profiles Over 120,000 Years of Ecosystem Development. *Frontiers in Microbiology, 8*(874). Original Research. https://www.frontiersin.org/article/10.3389/fmicb.2017.00874

Viscarra Rossel, R. A., Adamchuk, V. I., Sudduth, K. A., McKenzie, N. J., & Lobsey, C. (2011). Chapter Five - Proximal Soil Sensing: An Effective Approach for Soil Measurements in Space and Time. In D. L. Sparks (Ed.), *Advances in Agronomy* (Vol. 113, pp. 243-291): Academic Press.

Viscarra Rossel, R. A., McBratney, A. B., & Minasny, B. (2010). *Proximal Soil Sensing*: Springer Netherlands.

Vitousek, P., Chadwick, O. A., Matson, P., Allison, S., Derry, L., Kettley, L., et al. (2003). Erosion and the Rejuvenation of Weathering-derived Nutrient Supply in an Old Tropical Landscape. *Ecosystems, 6*(8), 762-772.

Vitousek, P., Dixon, J. L., & Chadwick, O. A. (2016). Parent material and pedogenic thresholds: observations and a simple model. *Biogeochemistry, 130*(1), 147-157. https://doi.org/10.1007/s10533-016-0249-x

Wardle, D. A., Walker, L. R., & Bardgett, R. D. (2004). Ecosystem Properties and Forest Decline in Contrasting Long-Term Chronosequences. *Science, 305*(5683), 509-513. http://www.sciencemag.org/cgi/content/abstract/305/5683/509

Webb, T. H., Campbell, A. S., & Fox, F. B. (1986). Effect of rainfall on pedogenesis in a climosequence of soils near Lake Pukaki, New Zealand. *New Zealand Journal of Geology and Geophysics, 29*(3), 323-334. https://doi.org/10.1080/00288306.1986.10422155

White, A. F., Blum, A. E., Schulz, M. S., Vivit, D. V., Stonestrom, D. A., Larsen, M., et al. (1998). Chemical Weathering in a Tropical Watershed, Luquillo Mountains, Puerto Rico: I. Long-Term Versus Short-Term Weathering Fluxes. *Geochimica et Cosmochimica Acta, 62*(2), 209-226. http://www.sciencedirect.com/science/article/pii/S0016703797003359

Wiesmeier, M., Urbanski, L., Hobley, E., Lang, B., von Lützow, M., Marin-Spiotta, E., et al. (2019). Soil organic carbon storage as a key function of soils - A review of drivers and indicators at various scales. *Geoderma, 333*, 149-162. https://www.sciencedirect.com/science/article/pii/S0016706117319845

689 Yoo, K., Amundson, R., Heimsath, A. M., Dietrich, W. E., & Brimhall, G. H. (2007). Integration of geochemical
690 mass balance with sediment transport to calculate rates of soil chemical weathering and transport on
691 hillslopes. *Journal of Geophysical Research: Earth Surface, 112*(F2), n/a-n/a.
692 http://dx.doi.org/10.1029/2005JF000402
693 Zhang, Y., Ji, W., Saurette, D. D., Easher, T. H., Li, H., Shi, Z., et al. (2020). Three-dimensional digital soil
694 mapping of multiple soil properties at a field-scale using regression kriging. *Geoderma, 366*, 114253.
695 https://www.sciencedirect.com/science/article/pii/S0016706119302125
696